

RESEARCH ARTICLE

10.1002/2017JD026774

Key Points:

- $\delta^{18}\text{O}_E$ of open-water evaporation was determined with the gradient-diffusion method at hourly intervals
- Results indicate a weak kinetic fractionation against ^{18}O in open-water evaporation
- The often-used kinetic parameter for lakes causes underestimation of the lake annual evaporation from the isotope mass balance method

Supporting Information:

- Supporting Information S1
- Data Set S1

Correspondence to:

W. Xiao and X. Lee,
wei.xiao@nuist.edu.cn;
xuhui.lee@yale.edu

Citation:

Xiao, W., Lee, X., Hu, Y., Liu, S., Wang, W., Wen, X., ... Xie, C. (2017). An experimental investigation of kinetic fractionation of open-water evaporation over a large lake. *Journal of Geophysical Research: Atmospheres*, 122, 11,651–11,663. <https://doi.org/10.1002/2017JD026774>

Received 23 MAR 2017





Accepted 25 OCT 2017

Accepted article online 30 OCT 2017

Published online 11 NOV 2017

©2017. American Geophysical Union.
All Rights Reserved.

An Experimental Investigation of Kinetic Fractionation of Open-Water Evaporation Over a Large Lake

Wei Xiao¹ , Xuhui Lee^{1,2} , Yongbo Hu¹, Shoudong Liu¹, Wei Wang¹, Xuefa Wen³ , Martin Werner⁴ , and Chengyu Xie¹

¹Yale-NUIST Center on Atmospheric Environment and Collaborative Innovation Center on Forecast and Evaluation of Meteorological Disasters, Nanjing University of Information Science and Technology, Nanjing, China, ²School of Forestry and Environmental Studies, Yale University, New Haven, CT, USA, ³Key Laboratory of Ecosystem Network Observation and Modeling, Institute of Geographic Sciences and Natural Resources Research, Chinese Academy of Sciences, Beijing, China, ⁴Alfred Wegener Institute, Helmholtz Centre for Polar and Marine Research, Bremerhaven, Germany

Abstract The oxygen isotopes of water (H_2^{18}O and H_2^{16}O) are tracers widely used for the investigation of Earth science problems. The tracer applications are based on the premise that the $^{18}\text{O}/^{16}\text{O}$ ratio of open-water evaporation ($\delta^{18}\text{O}_E$) can be calculated from environmental conditions. A long-standing issue concerns the role of kinetic fractionation, or diffusion transport, in the evaporation process. Here we deployed an optical instrument at a large lake (area 2,400 km²) to make in situ measurement of $\delta^{18}\text{O}$ and δD of atmospheric vapor, then determined $\delta^{18}\text{O}$ and δD of open-water evaporation using the gradient-diffusion method. Our results show a much weaker kinetic effect than suggested by the kinetic factor ε_k adopted in some previous studies of lake hydrology (14.2‰). By incorporating into the H_2^{18}O isotopic mass balance of the lake a lower ε_k value (about 6.2‰) used for ocean evaporation in global climate models, we obtain an annual lake evaporation rate that agrees with an independent eddy-covariance observation, but the rate is 72% higher than if the commonly used lake ε_k value of 14.2‰ is applied. The applicability of this results to small lakes is uncertain and in need of field-based assessment.

1. Introduction

Lakes are precious water resources for the society. They play an important part in regulating regional weather and climate. The evaporative water loss to the atmosphere is one of the primary factors controlling lake water level, and although a small contributor to the overall terrestrial flux to the atmosphere (Gibson & Reid, 2014), represents a water source that can enhance local precipitation by up to 100% near large lakes (Scott & Huff, 1996). Direct measurement of lake evaporation is challenging because of logistical difficulty, especially for deep lakes (Blanken et al., 2011). Numerical predictions of lake evaporation remain uncertain due to the difficulties in predicting lake freeze and thaw dates and thermal diffusion in the water column (Subin et al., 2012). An alternative approach based on the isotopic balance can overcome these difficulties.

In the surface evaporation process, the heavier H_2^{18}O molecules escape at a lower relative rate than the lighter H_2^{16}O molecules, resulting in depletion of H_2^{18}O in atmospheric vapor and enrichment in lake and oceanic waters (e.g., Jouzel et al., 2013). The degree of preferential depletion and enrichment is dictated by environmental conditions under which the evaporation takes place (Craig & Gordon, 1965). These conditions are imprinted on the atmospheric water cycle at the time of evaporation, providing powerful constraints on lake evaporation rates (Gibson et al., 2016, 2017; Jasechko et al., 2014) and local water recycling (Bowen et al., 2012; Gat et al., 1994; Machavaram & Krishnamurthy, 1995), enabling reconstruction of past climate conditions from ice cores (Jouzel et al., 2007; Steffensen et al., 2008), and providing independent evaluation of parameterizations in models of large-scale atmospheric dynamics and convective cloud formation (Lee et al., 2009; Noone & Sturm, 2010; Sherwood & Risi, 2012).

The kinetic effect, an important part of the overall evaporative fractionation against H_2^{18}O , has been a subject of debate for more than half a century. The kinetic effect arises because the H_2^{18}O molecules diffuse more slowly in the atmosphere than the H_2^{16}O molecules. The strength of the kinetic effect is measured by the kinetic fractionation factor ε_k , defined as the deviation from unity of the H_2^{16}O to H_2^{18}O diffusivity ratio and expressed in parts per thousand or ‰. The molecular diffusivities of vapor isotopes cannot be quantified precisely with the classic kinetic theory (Luz et al., 2009). Laboratory determination of their diffusivities is

hampered by sensitivity to humidity perturbation (Barkan & Luz, 2005) and evaporative cooling (Cappa et al., 2003) and isotopic enrichment (Kim & Lee, 2011) of the water surface. In the outdoor environment, the diffusion pathway consists of a water-air interfacial layer and a turbulent atmospheric surface layer (the air layer extending from the surface to a height of about 10 m; Craig & Gordon, 1965). Because turbulent diffusion does not discriminate against H_2^{18}O or H_2^{16}O , the overall ϵ_k of open-water evaporation is lower than that associated with molecular diffusion alone.

Here opinions diverge on how to best incorporate the role of atmospheric turbulence. By adopting a parameterization for turbulence in the interfacial layer, some terrestrial hydrologists decrease the molecular ϵ_k by half, to 14.2‰ for H_2^{18}O , to describe lake evaporation (Gonfiantini, 1986), meaning that the heavier H_2^{18}O molecules diffuse 14.2‰ more slowly in ambient air than the lighter H_2^{16}O molecules. This lake ϵ_k value (14.2‰), which is used in the analysis presented below, represents the lower bound of the lake parameterizations found in most of the terrestrial hydrology literatures (e.g., Gibson et al., 1996, 2016; Horita et al., 2008; Isokangas et al., 2015; Jasechko et al., 2014; Krabbenhoft et al., 1990). It is the default used in a popular lake isotope calculator for lakes of all sizes (Skrzypek et al., 2015). In the study of global land surface evaporation by Jasechko et al. (2013), the same value is used for both large lakes and small lakes. Furthermore, it is used in a recent study of isotopic mass balance of the Great Lakes (Jasechko et al., 2014).

The kinetic fractionation factor for soil evaporation is soil moisture dependent (Mathieu & Bariac, 1996) and that for plant transpiration is weighted by the stomatal and the boundary layer resistances (Farquhar & Lloyd, 1993), and both are generally larger than the default lake value used here.

In global climate models (GCMs), ϵ_k is weakly dependent on wind and is reduced further from the molecular value to about 6.2‰ for H_2^{18}O for oceanic evaporation under smooth conditions (Sturm et al., 2010). This formulation accounts for an additional turbulent diffusion resistance in the atmospheric surface layer, which represents about two thirds of the overall diffusion resistance (Merlivat & Jouzel, 1979).

Both the lake (LK) and the ocean surface (OS) approaches are approximations, and so far have not been validated directly against in situ field measurement of the isotopic evaporation flux from lake waters even though some recent studies over the oceans support the OS approach (Benetti et al., 2014; Steen-Larsen et al., 2014). The choice of whether to use the LK or the OS ϵ_k has important consequences. For instance, as we will demonstrate later, they result in a totally opposite conclusion about whether lake evaporation acts to enhance or to reduce the H_2^{18}O abundance of atmospheric water.

In this paper, we report the results of an experimental determination of $\delta^{18}\text{O}_E$ of open-water evaporation. The experimental site was Lake Taihu, a large lake in eastern China (area 2,400 km²). Measurements of $^{18}\text{O}/^{16}\text{O}$ ratios of atmospheric water vapor (δ_v) were made with an in situ optical instrument, and the isotopic ratio of lake evaporation flux ($\delta^{18}\text{O}_E$) was determined with the gradient-diffusion method. We aim to determine which of the two kinetic factors (LK versus OS) is more appropriate for describing the lake isotopic process. Evaluation of the two different kinetic parameter values was achieved by comparing the observations with the Craig-Gordon model prediction of $\delta^{18}\text{O}_E$ (Craig & Gordon, 1965). We also discuss the implication of the kinetic effect for the determination of lake evaporation using the isotope mass balance principle.

2. Materials and Methods

2.1. In Situ Measurement of Isotopic Evaporation

2.1.1. Experimental Site and Instrument

The experimental site was part of the Taihu Eddy Flux Network (Lee et al., 2014). Lake Taihu is a large (area 2,400 km²) and shallow (mean depth 1.9 m) freshwater lake located in the Yangtze River Delta, China (Figure 1). The H_2O , H_2^{18}O , and HDO concentration differences over the lake were measured with an isotope water vapor analyzer (Model 911-0004; Los Gatos Research, Mountain View, CA, USA). A schematic design diagram of the gradient measurement system is shown in Figure 2. The air intakes were located at approximately 1.1 and 3.5 m above the water surface and at a distance of 250 m from the shore. The analyzer and the vapor calibration source were housed in a small temperature-controlled instrument shed at the end of an elevated boardwalk. All sampling parts were made of Teflon material. The analyzer was a custom-designed model with an improved instrument response time and a fast sample flow rate (0.4 L min⁻¹ at STP and about 8 L min⁻¹ at the cell operation pressure of about 50 hPa). The instrument response was further improved by using a very

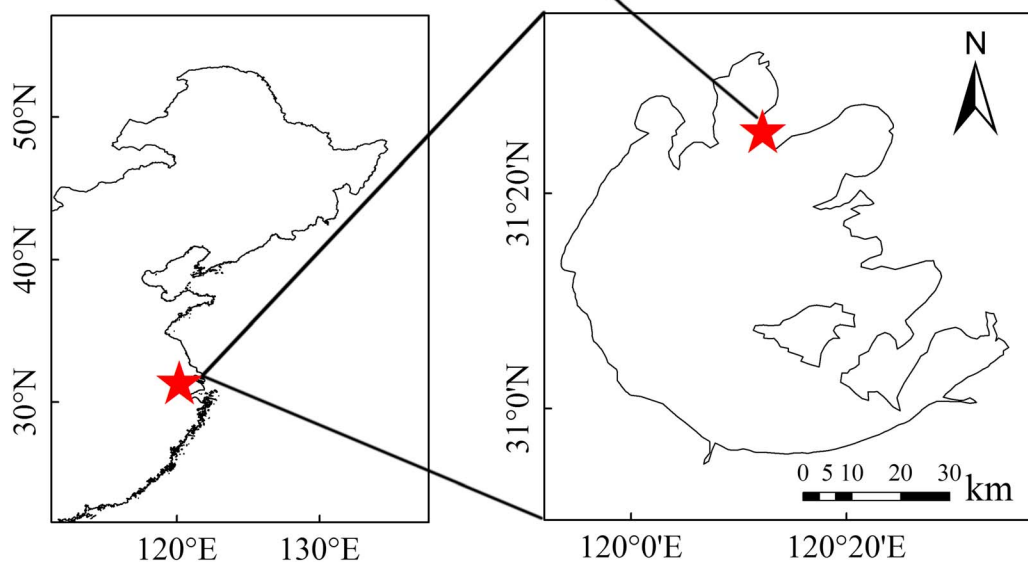


Figure 1. Map and photograph showing the measurement site at Lake Taihu.

small (ID 0.32 cm) and short tube (length 0.65 m) between the common port of the manifold and the analyzer. All the sampling parts upstream of the analyzer were heated at 5 to 10 K above the environmental temperature to minimize tube wall effects and to avoid condensation.

The H_2O , H_2^{18}O , and HDO mixing ratios at the two heights were measured by switching between the two intake tubes at 30 s intervals. Figure 3 presents a data sequence showing step changes of the measurement in response to valve switching. The measurement approached steady state in less than 10 s after each switching. To avoid the memory effect after valve switching, the first 20 data points (20 s) after each valve switching were excluded in the determination of the vertical mixing ratio differences between the two measurement heights.

The calibration vapor was generated by a vapor source supplied with a working liquid water standard (Model 908-0003-9002; Los Gatos Research, Mountain View, CA, USA) traceable to the VSMOW scale. Every 3 h, the

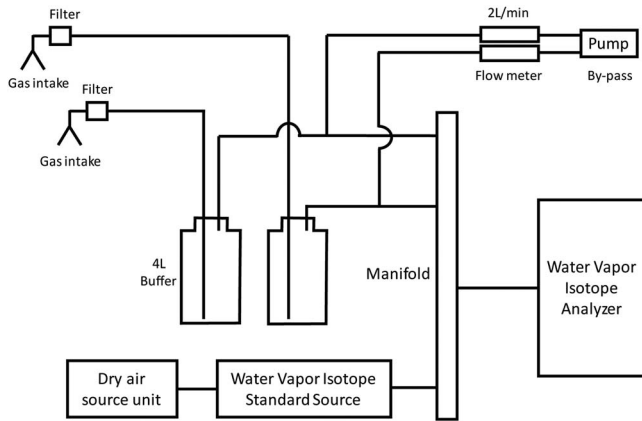


Figure 2. Schematic design diagram of the gradient measurement system.

analyzer sampled the calibration vapor at five different humidity levels (Figure 4), two of which that bracketed the ambient air humidity were selected for calibration. The first 180 data points (3 min) after each valve switching were excluded from the instrument calibration.

The experiment period was 4 August 2012 to 15 November 2014. The high-frequency (1 Hz) data were averaged to hourly intervals. Our analysis of the kinetic fractionation effect relied mainly on observations made under open fetch conditions (8 to 50 km, the distance between the measurement location and the nearest shoreline upwind), in which wind blew from the lake with wind directions 140°–315° and at a mean speed of 3.4 m s⁻¹ (Figure 1). The fetch was large enough to avoid the effect of advection. All isotopic compositions are expressed in the delta notation in reference to the Vienna SMOW scale.

2.1.2. Calibration of the Vapor Isotope Measurement

Here we describe briefly the method used to calibrate the vapor isotopic measurement. Full details of the method can be found in the study of Wen et al. (2008) and in the supporting information. First, the measured molar mixing ratio of the major and the minor isotopologue was corrected for gain errors using the measurement of the calibration vapor. The gain correction was done twice by using two calibration vapor streams, one of which (s1) had slightly lower humidity and the other (s2) slightly higher humidity than the ambient sample being measured. These gain-corrected delta values are denoted as δ_1 and δ_2 .

Next, a two-point interpolation was used to remove the concentration dependence as

$$\delta_V = \delta_1 + \frac{\delta_2 - \delta_1}{x_{s,2} - x_{s,1}} (x_a - x_{s,1}) \tag{1}$$

where δ_V is the true ¹⁸O/¹⁶O ratio in delta notation of the ambient vapor and x_a , $x_{s,1}$, and $x_{s,2}$ are the molar mixing ratio of the ambient sample, calibration stream s1, and calibration stream s2, respectively. An example of the concentration dependence is given in Figure S1 in the supporting information.

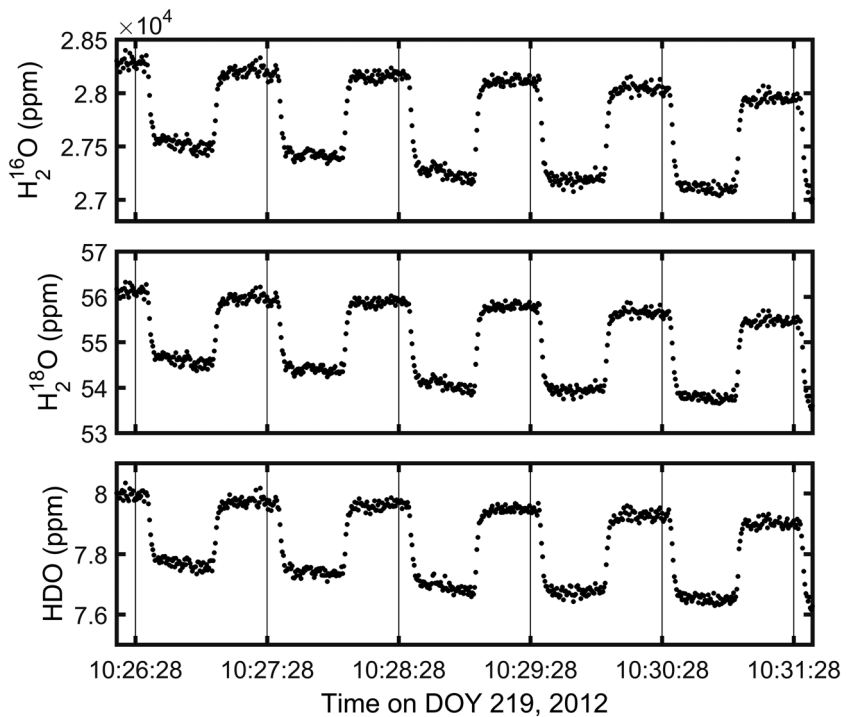


Figure 3. Step changes in the H₂O, H₂¹⁸O, and HDO mixing ratios in response to valve switching.

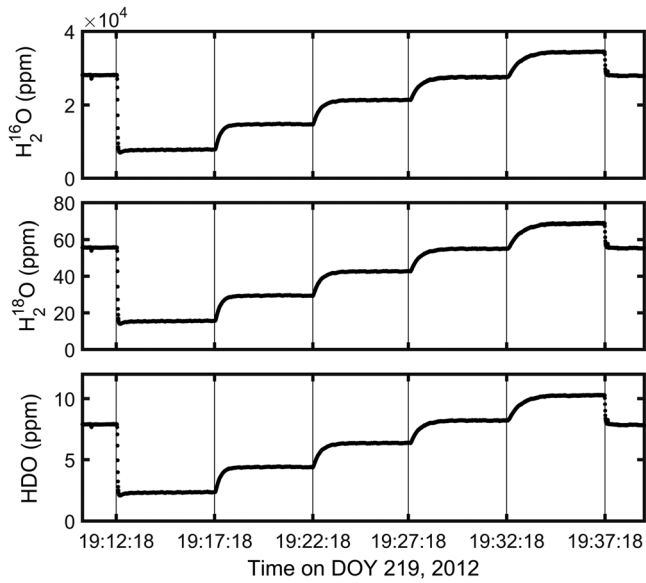


Figure 4. Step changes in the H₂O, H₂¹⁸O, and HDO mixing ratios during a calibration cycle.

The importance of in situ calibration is evident in Figure S2 in the supporting information. Without the calibration, the instrument bias errors can be as large as 80‰ for D/H and 20‰ for ¹⁸O/¹⁶O. After calibration, the bias errors are reduced to within ±2‰ for D/H and within ±0.2‰ for ¹⁸O/¹⁶O. With comparison to our water standard, the bias of the isotopic water vapor measurement is 0.1 ± 0.6‰, 0.2 ± 0.3‰, and 0.1 ± 0.2‰ for δ¹⁸O and 0.8 ± 1.7‰, -0.1 ± 1.0‰, and -0.1 ± 1.0‰ for δD at low (1.2 ± 0.2%Volume), medium (1.6 ± 0.3%Volume), and high water vapor mixing ratios (2.0 ± 0.4%Volume), respectively.

Our calibration strategy is different from that used for isotope-ratio mass spectrometer analysis. In the latter case, two or more isotope standards are used to bracket the delta value of the sample. Here the calibration procedure was made with a single isotope ratio but with two or more concentration values to bracket the concentrations of both the major and minor species in the ambient sample. In real-time atmospheric measurements, changes in the vapor concentrations are very large, and we found that it is necessary to use a time-varying calibration in order to remove concentration dependence. We have done extensive tests of this procedure for a number of commercial analyzers, including the type used in the present study, by checking against independent working vapor standards whose isotopic compositions are very different

from those used for the calibration water feed. The results show that after calibration these instruments achieve precision and accuracy comparable to those of isotope ratio mass spectrometry (Lee et al., 2005; Wen, Lee, Sun, Wang, Hu, et al., 2012).

2.1.3. Determination of the Isotopic Ratio of Evaporation

The evaporation isotopic compositions were determined with the gradient-diffusion method. This technique was first described by Lee et al. (2007) and has since been used in several other studies on isotopic compositions of land evaporation (Santos et al., 2014; Welp et al., 2008; Wen, Lee, Sun, Wang, Tang, et al., 2012) and later improved with the use of the latest generation of laser-based optical spectroscopy technology (Wen et al., 2016).

Let $\hat{x}_{a,1}$ and $\hat{x}'_{a,1}$ be the true molar mixing ratios of the major and the minor vapor isotopologue measured at height 1 above the water surface and $\hat{x}_{a,2}$ and $\hat{x}'_{a,2}$ be the true molar mixing ratios at height 2. According to the gradient-diffusion theory, the molar D/H or ¹⁸O/¹⁶O ratio of evaporation is given

$$R_E = \frac{\hat{x}'_{a,1} - \hat{x}'_{a,2}}{\hat{x}_{a,1} - \hat{x}_{a,2}} \quad (2)$$

Because the measurement was made close to the surface and at sufficient distances from the lakeshore, the observed vertical difference in the vapor molar mixing ratio were driven only by lake evaporation (Garratt, 1992). Equation (2) makes four assumptions: (1) that air in the surface layer above the lake is fully turbulent so that diffusion is equally efficient among the isotope species, (2) the fluxes are constant with height, (3) the horizontal gradients of the mixing ratios are negligible, and (4) the atmosphere is in steady state so that changes in storage of water vapor below the measurement heights can be omitted.

Equation (2) is equivalent to

$$R_E = R_s \cdot \frac{x_{s,2} - x_{s,1}}{x'_{s,2} - x'_{s,1}} \cdot \frac{x'_{a,2} - x'_{a,1}}{x_{a,2} - x_{a,1}} \quad (3)$$

where R_s is the molar D/H or ¹⁸O/¹⁶O ratio of the calibration water, $x_{s,1}$ and $x'_{s,1}$ are uncalibrated molar mixing ratios of the major and the minor vapor isotopologue of calibration vapor stream s1, and $x_{s,2}$ and $x'_{s,2}$ are uncalibrated mixing ratios of the major and the minor vapor isotopologue of calibration vapor stream s2 (Lee et al., 2007). Details of the derivation of equation (3) are given in the supporting information. Observations whose H₂O mixing ratio difference was smaller than 200 ppm were excluded from the calculation of the evaporation delta values to avoid errors from division of small numbers.

The molar ratio is converted to the delta scale to give the isotopic composition of evaporation in delta notation, as

$$\delta_E = (R_E/R_{VSMOW} - 1) \times 1000 \quad (4)$$

where R_{VSMOW} is the molar D/H or $^{18}\text{O}/^{16}\text{O}$ ratio of the Vienna standard mean ocean water (VSMOW), with values of 0.00015576 for D/H and 0.0020052 for $^{18}\text{O}/^{16}\text{O}$.

2.2. The Craig-Gordon Model

The Craig-Gordon model appears in several different forms in the published literature, mostly due to different ways of expressing the kinetic effect. The form used in this study (equation (5) below) is a common usage in oceanic and global climate model studies (Dee et al., 2015; Hoffmann et al., 1998; Merlivat & Jouzel, 1979; Pfahl et al., 2012; Risi et al., 2010) and by terrestrial ecologists (e.g., the review by Yakir & Sternberg, 2000). In this form of the model, the humidity influence is expressed explicitly, and the kinetic factor ϵ_k is independent of humidity. In some lake experimental studies, the kinetic factor is defined differently from equation (5). In Text S2 in the supporting information, we will show that our results apply equally well to both.

We used the Craig-Gordon model to calculate the isotopic compositions of the lake evaporation (δ_E)

$$\delta_E = \frac{\alpha_{\text{eq}}^{-1} \delta_L - h \delta_V - \epsilon_{\text{eq}} - (1 - h) \epsilon_k}{1 - h + 10^{-3} (1 - h) \epsilon_k} \quad (5)$$

(Yakir & Sternberg, 2000), where $\alpha_{\text{eq}} (>1)$ is the equilibrium fractionation factor calculated from the lake water surface temperature (Majoube, 1971), $\epsilon_{\text{eq}} = (1 - 1/\alpha_{\text{eq}}) \times 10^3$, ϵ_k is the kinetic fractionation factor, h is relative humidity in reference to the lake surface temperature, δ_V is vapor isotopic composition in the atmospheric surface layer above the lake, and δ_L is the lake liquid water isotopic composition. The vapor isotope ratio (δ_V) was measured at hourly intervals using the optical instrument; water surface temperature and air humidity were measured at 30 min intervals by a suite of micrometeorological instruments (Lee et al., 2014), and the lake water delta was measured with water sampled daily at a depth of 20 cm.

The isotopic compositions of the lake water column are well mixed because convective overturning is commonplace at this shallow lake. Profile measurement made from August 2011 to May 2012 indicates that the difference between the surface and the 1.5 m depth was less than 0.1‰ for $\delta^{18}\text{O}$ and less than 0.2‰ for δD . So the Craig-Gordon model deployed here was free of the artifacts associated with isotopic enrichment of the surficial water as observed in laboratories and with evaporation pans (Kim & Lee, 2011) and with isotopic stratification in deep lakes and in the ocean (Craig & Gordon, 1965).

The model was used at three different time scales. At the hourly time scale, two sets of calculation were performed. In one set of calculation, we deployed the LK kinetic factor used for lake studies (14.2‰ for H_2^{18}O and 12.5‰ for HDO; Gonfiantini, 1986; Horita et al., 2008). In the second set of calculations, the OS kinetic factor was parameterized as a weak function of wind speed and for the measurement height of 3.5 m, with a mean value of 6.2‰ for H_2^{18}O and 5.5‰ for HDO. (According to the diffusion theory of Merlivat & Jouzel, 1979, ϵ_k is not sensitive to height: elevating the reference height to a standard height of 10 m decreases ϵ_k slightly by about 0.5‰.) The atmospheric input variables (δ_V and h) were measured at the upper level (3.5 m), the same height for which the OS ϵ_k was calculated. The δ_E calculated with the model (equation (5)) was then compared with the hourly δ_E determined with the gradient-diffusion method (equation (3)).

At the 5 day time scale, the delta values calculated at hourly time steps from equation (5) were weighted by the evaporation flux measured with an eddy covariance system at the site to obtain a single δD_E and $\delta^{18}\text{O}_E$. These 5 day delta values of evaporation were compared with the local evaporation line (LEL). In this study, fourteen 5 day periods with continuous δ_V measurement were selected for this analysis. The LEL was obtained by linearly regressing the HDO and H_2^{18}O compositions of the lake water measured over the same time periods.

At the annual time scale, δ_E was calculated at a time step of 1 month. Monthly δ_E was calculated using the Craig-Gordon model with monthly input variables (δ_V , h , wind speed, and water surface temperature). Data gaps in δ_V were filled with a regression that expresses δ_V as a function of atmospheric water vapor mixing

ratio. The monthly δ_E was weighted by monthly net radiation flux to obtain annual δ_E , which was used for the lake isotope mass balance analysis as described below.

An advantage of equation (5) is that it explicitly expresses the humidity influence, so the kinetic factor ε_k is independent of humidity. In some lake experimental studies, the kinetic factor is defined differently from equation (5). In Text S2 in the supporting information, we show that our results apply equally well to both.

2.3. Isotopic Mass Balance of the Lake

To further evaluate the kinetic effect, we compared the lake evaporation rate calculated from the lake isotopic mass balance with that measured directly by eddy covariance. The isotopic mass balance method was applied to the annual period from October 2013 to September 2014, as

$$E = \frac{V \frac{d\delta_L}{dt} + (\delta_L - \delta_Q) \frac{dV}{dt} + I(\delta_Q - \delta_I)}{\delta_Q - \delta_E} \quad (6)$$

(Dincer, 1968), where E is lake evaporation, V is lake water volume, I is the total input rate (the sum of inflow river runoff volumes and precipitation), groundwater contribution as an input is not considered here, t is time, δ_Q and δ_I are the isotopic compositions of outflow river water and incoming water, respectively. Equation (6) is a solution to the H_2^{18}O mass balance equation and the water budget equation of the lake. The runoff volumes of inflow rivers and time variation of the lake water volume were obtained from monthly reports prepared by the Taihu Basin Authority. Precipitation was the mean value of the observations at three meteorological stations near the lake (Wuxi, Huzhou, and Dongshan). The isotopic composition of evaporation was computed by the Craig-Gordon model as described above. The isotopic compositions of the lake water, inflow rivers, and outflow rivers were obtained from water samples collected once per season in February, May, August, and November and were amount-weighted (Xiao et al., 2016). Because we did not sample precipitation during the experimental period, the isotopic composition of precipitation was calculated according to an empirical model established at an experimental site nearby (Liu et al., 2014). Lake water samples were collected at 29 sites evenly distributed across the whole lake. Water samples were collected from 51 rivers at 100 m from the river-lake confluence. The isotopic compositions of lake water and river water samples were analyzed using a liquid water isotope analyzer (Model DLT-100; Los Gatos Research, Mountain View, CA, USA), and the measurement precision was $\pm 0.3\text{‰}$ for δD and $\pm 0.1\text{‰}$ for $\delta^{18}\text{O}$. Uncertainty estimates for the isotopic budgets were made with a Monte Carlo procedure employing a Gaussian distribution for error in the input variables and an ensemble of 800,000 realizations.

3. Results

3.1. Isotopic Compositions of Lake Evaporation at Hourly Intervals

Figure 5 compares the hourly $\delta^{18}\text{O}_E$ calculated with the Craig-Gordon model with the observed value. Both the model results and the observations show large hour-to-hour variability in $\delta^{18}\text{O}_E$ (Figures 5a and 5d) and notable diurnal variations (Figure 5c). During the whole measurement period, the observed $\delta^{18}\text{O}_E$ under open fetch conditions varied from -29.9‰ to 8.8‰ , with a mean value of -14.1‰ . A significant contributor to this variability was temporal changes in relative humidity. The linear correlation between $\delta^{18}\text{O}_E$ and h was 0.35 (number of observations = 539, $p < 0.01$).

The Craig-Gordon model performed much better if we used the OS ε_k than the LK value. Using the OS ε_k , $\delta^{18}\text{O}_E$ calculated using the Craig-Gordon model agreed well with the observation (Figure 5a), with an index of agreement (IA) of 0.87, a root-mean-square error (RMSE) of 4.2‰ , and a mean error (ME) of 0.9‰ . If the LK ε_k was used, the $\delta^{18}\text{O}_E$ was underestimated (Figure 5b), with a lower IA of 0.72, a larger RMSE of 7.4‰ , and a large and negative ME of -6.2‰ .

The diurnal composite time series indicate that the Craig-Gordon model captured the diurnal variability of $\delta^{18}\text{O}_E$ (Figure 5c), but with different bias errors depending on the ε_k value used. Using the OS ε_k , the modeled $\delta^{18}\text{O}_E$ during midday agreed well with the observation. The mean values of observed and modeled $\delta^{18}\text{O}_E$ during midday (10:00–14:00 LST) were -14.1‰ and -14.3‰ , respectively. If the LK ε_k was used, the modeled midday mean value was much lower, at -21.3‰ . The OS parameterization showed some biases for night hours (Figure 5c), either because of difficulties in measuring $\delta^{18}\text{O}_E$ in low flux conditions or because the parameterization itself is not precise enough for a statically stable atmosphere.

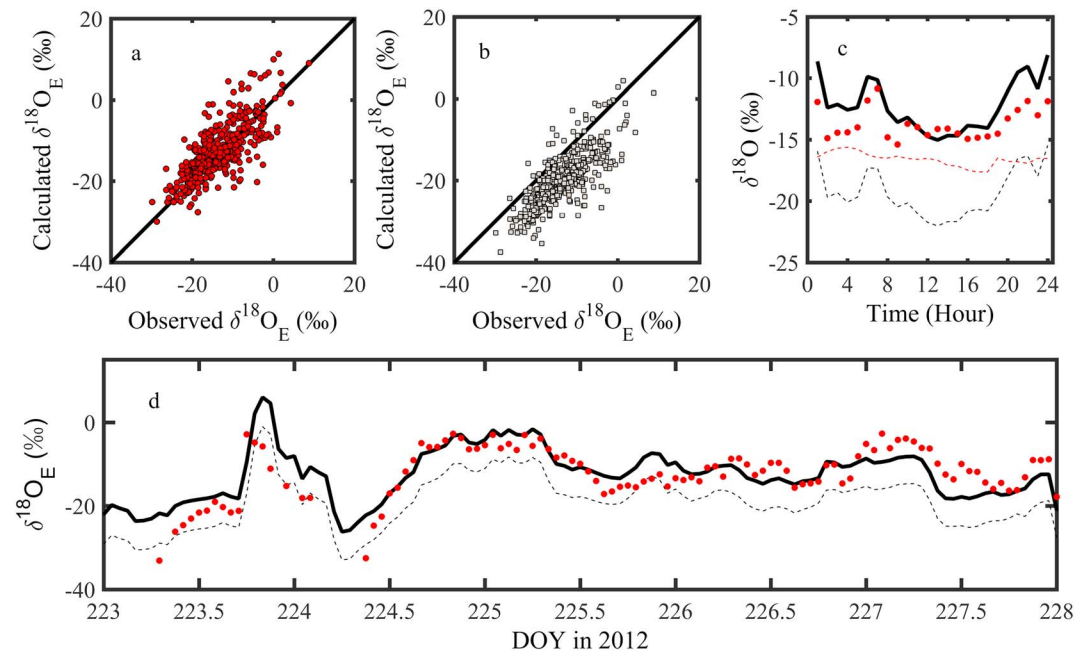


Figure 5. H_2^{18}O isotopic composition of evaporation at Lake Taihu under open fetch conditions. (a) Comparison of the Craig-Gordon model calculations with the OS ϵ_k against the observations. (b) Comparison of the Craig-Gordon model calculations with the LK ϵ_k against the observations. (c) Diurnal composite of $\delta^{18}\text{O}_E$ calculated with the OS ϵ_k (solid line) and the LK ϵ_k (black dashed line), the observed $\delta^{18}\text{O}_E$ (red dots), and the observed H_2^{18}O composition of water vapor (red dashed line). (d) Time series of $\delta^{18}\text{O}_E$ calculated with the OS ϵ_k (solid line) and the LK ϵ_k (dashed line), and the observed $\delta^{18}\text{O}_E$ (red dots). The solid lines in Figures 5a and 5b are 1:1 match.

Another noteworthy point is the contrast between the observed vapor $^{18}\text{O}/^{16}\text{O}$ ratio ($\delta^{18}\text{O}_V$) and the observed and modeled $\delta^{18}\text{O}_E$. The observed $\delta^{18}\text{O}_E$ is higher than $\delta^{18}\text{O}_V$ by an average amount of 3.1‰. The mean difference was 2.6‰ at midday and 3.8‰ at night (22:00–02:00 LST). The OS parametrization predicts that $\delta^{18}\text{O}_E$ should be higher than $\delta^{18}\text{O}_V$, in agreement with the observation (Figure 5c), implying that the lake evaporation should enrich the atmospheric water with H_2^{18}O . But the LK parameterization led to a totally opposite conclusion.

In the case of the stable hydrogen isotopes, both parameterizations yielded excellent agreement with the observed deuterium (HDO) composition of the lake evaporation (δD_E ; Figure S3 in the supporting information). The lack of δD_E sensitivity to ϵ_k (with the OS value of 5.5‰ and the LK value of 12.5‰) is not surprising, since evaporative fractionation against HDO is dominated by the equilibrium fractionation mechanism. Both calculations indicate that the lake evaporation should enrich the atmospheric water with HDO: the calculated δD_E was greater than the HDO composition of atmospheric water vapor (δD_V). This is in agreement with the observations and with the results obtained for H_2^{18}O showing that the observed δD_E and $\delta^{18}\text{O}_E$ were greater than δD_V and $\delta^{18}\text{O}_V$, respectively (Figure S3 in the supporting information and Figure 5).

3.2. The HDO- H_2^{18}O Relationship

Evidence for a weak kinetic effect is also seen in the HDO- H_2^{18}O relationship. In the HDO- H_2^{18}O parameter space, the isotopic compositions of the lake water should fall below the global meteoric water line (GMWL) and those of the evaporated vapor above the GMWL, due to the evaporative enrichment and depletion of these isotopes in the liquid and the vapor phase, respectively. Mass balance requires that the evaporation delta values be on the LEL defined by the lake water delta values (Gibson et al., 1993). Using the OS ϵ_k , the calculated 5 day evaporation delta values varied from -149.3‰ to -46.7‰ for δD_E and -22.6‰ to -5.7‰ for $\delta^{18}\text{O}_E$ (Figure 6). If the LK ϵ_k was used in the model calculation, the range of variation was -154.4‰ to -52.7‰ for δD_E and -29.3‰ to -12.8‰ for $\delta^{18}\text{O}_E$. Generally, the evaporation delta values calculated with the OS ϵ_k followed closely with the LEL, while those calculated with the LK ϵ_k deviated systematically from the LEL. After being weighted by the evaporation flux, the mean δD_E and $\delta^{18}\text{O}_E$ of all the 5 day values (-94.4‰

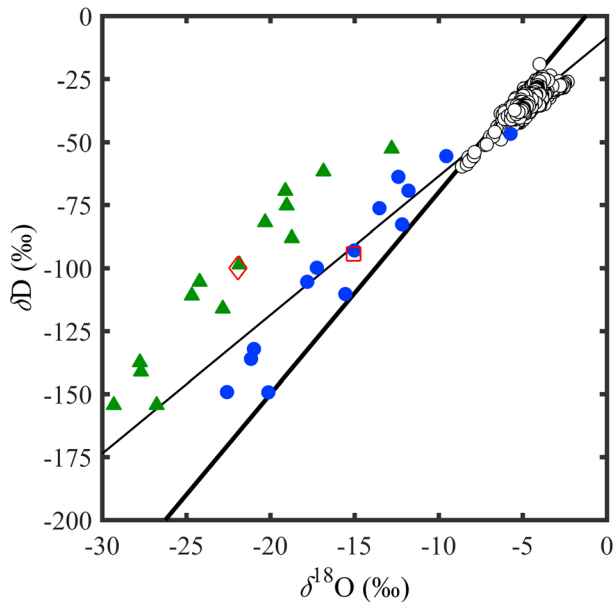


Figure 6. Comparison of the Craig-Gordon model calculation with the local evaporation line. Lake water isotopic compositions are denoted as white dots, and isotopic compositions of lake evaporation calculated by the model with the OS ϵ_k and with the LK ϵ_k are denoted as blue dots and green triangles, respectively. Each solid symbol represents 5 day mean values weighted by the evaporation flux. The overall flux weighted isotopic compositions are denoted by the open square (OS ϵ_k) and the open diamond (LK ϵ_k). The thin line is the local evaporation line (LEL), and the thick line represents the global meteoric water line (GMWL). For reference, the local mean precipitation water line for this region is $\delta D = 8.77\delta^{18}O + 13.96$ (Liu et al., 2014).

$20.3 \pm 1.9 \times 10^8 \text{ m}^3 \text{ water yr}^{-1}$ or $846 \pm 79 \text{ mm yr}^{-1}$ with the LK ϵ_k . The low sensitivity to the kinetic fractionation against HDO was consistent with the Craig-Gordon model results at hourly time steps (Figure S3 in the supporting information). In this regard, HDO may be a better tracer than H_2^{18}O isotope for the mass balance approach to study lake evaporation.

versus -15.1‰) fell almost exactly on the LEL (open square, Figure 6). But the LK ϵ_k caused the flux-weighted $\delta^{18}\text{O}_E$ to shift from the LEL by -5.3‰ (open diamond, Figure 6).

We used here the 5 day flux-weighted evaporation delta values for the LEL analysis so as to minimize the effect of extreme hourly values in low flux conditions, such as those obtained at nighttime. If hourly values were used in this analysis, the results obtained with the OS ϵ_k showed a small deviation from the LEL, but the deviation was still smaller than those obtained with the LK ϵ_k (Figure S4 in the supporting information).

3.3. Lake Evaporation Calculated From the Isotopic Mass Balance

The isotopic mass balance analysis revealed that the lake evaporation rate was very sensitive to the kinetic factor chosen for ^{18}O (Figure 7). A higher ϵ_k would lead to a greater amount of H_2^{18}O accumulated in the lake. In order to maintain the lake H_2^{18}O mass balance, the lake evaporation rate would have to be lowered. Based on the isotopic water balance (Dincer, 1968) and the OS ϵ_k , we estimated that Lake Taihu evaporated a total amount of $21.5 \pm 3.1 \times 10^8 \text{ m}^3 \text{ water yr}^{-1}$ (mean ± 1 standard deviation) or $896 \pm 129 \text{ mm yr}^{-1}$ to the atmosphere from October 2013 to September 2014. This amount is 72% greater than if the LK ϵ_k was used ($12.5 \pm 1.7 \times 10^8 \text{ m}^3 \text{ water yr}^{-1}$ or $521 \pm 71 \text{ mm yr}^{-1}$). For comparison, the evaporation rate observed with an eddy-covariance system was 863 mm yr^{-1} . The annual mean isotopic composition of lake evaporation calculated using the LK ϵ_k was $-20.4 \pm 2.0\text{‰}$, which is 7.0‰ lower than that calculated using the OS ϵ_k ($-13.4 \pm 1.3\text{‰}$).

If HDO was used as a tracer, the lake evaporation rate was $22.4 \pm 2.3 \times 10^8 \text{ m}^3 \text{ water yr}^{-1}$ or $933 \pm 96 \text{ mm yr}^{-1}$ with the OS ϵ_k and

4. Discussion

4.1. Height Dependence and Sensitivity of δ_V

Strictly, to be consistent with the Craig-Gordon model formulation, the vapor isotope ratio δ_V should be measured in the free air layer. In our calculation, we used atmospheric measurements of δ_V at the 3.5 m height as input to the Craig-Gordon model. This is justified because the vertical differences of these quantities are mostly restricted in the air layer very close to the surface (in the lower 1 m or less) due to the fact that water surfaces are aerodynamically very smooth. Field measurements revealed that the vapor isotope ratio is not sensitive to height. For example, Craig and Gordon (1965) found that the difference in the vapor $^{18}\text{O}/^{16}\text{O}$ ratio near the ocean surface (1–3 m) and at a mast height (13 m) is less than 0.12‰ . Gat et al. (2003) reported an $^{18}\text{O}/^{16}\text{O}$ ratio difference of 0.08‰ between two measurement heights (20.35 m versus 27.9 m) over the Mediterranean Sea. At Lake Taihu, the hourly $^{18}\text{O}/^{16}\text{O}$ ratio difference between the lower (1.1 m) and the upper intake (3.5 m) ranged from -0.78‰ to 0.81‰ , with a mean value of only 0.05‰ .

It is worth noting that the mass fluxes of the major and minor isotopes are driven by their respective mixing ratio gradients, which were generally

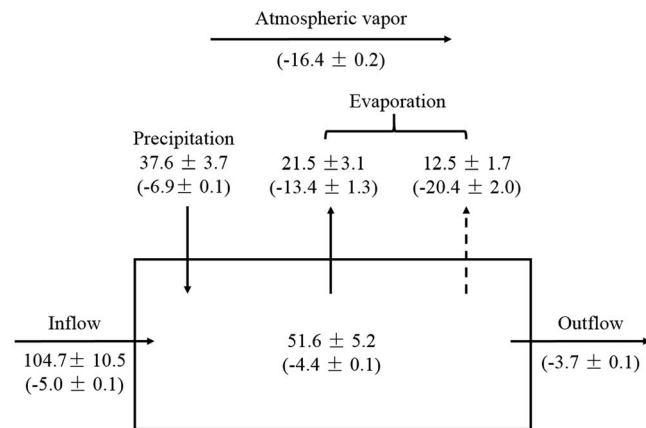


Figure 7. The isotopic mass balance of Lake Taihu from October 2013 to September 2014. The numbers outside the parentheses are water amounts ($\times 10^8 \text{ m}^3$). The numbers in the parentheses are the H_2^{18}O composition (‰). Two evaporation calculations are indicated by a solid arrow (OS ϵ_k) and a dashed arrow (LK ϵ_k). The change in lake water volume and its isotopic composition over this annual period are $9.1 \times 10^8 \text{ m}^3$ and -0.9‰ .

large (e.g., Figure 3), and not by the gradient of the vapor isotope ratio. We can have a situation where the vapor isotope delta difference between the two measurement heights is very small, but as long as the differences in the mixing ratios are large enough, equation (3) can be used to determine the flux isotope ratio.

In this study, the measurement of δ_V at the upper level (3.5 m) was used as the Craig-Gordon model input. Using the δ_V measured at the lower level (1.1 m), the calculated δD_E would be higher by $0.61 \pm 1.85\text{‰}$ (mean \pm one standard deviation) and the $\delta^{18}O_E$ would be higher by $0.59 \pm 0.48\text{‰}$. Figure S4 compares the δD_E and $\delta^{18}O_E$ relationships between the two calculations. We consider the calculation made with the 3.5 m measurement to be more accurate because this height is closer to the free air layer (Text S2 in the supporting information).

4.2. Large Lakes Versus Small Lakes

Several lines of evidence presented above point to a weak kinetic fractionation of evaporation against ^{18}O at Lake Taihu. Matching the Craig-Gordon model prediction with the $\delta^{18}O_E$ observed at hourly intervals requires a small OS kinetic factor of about 6.2‰ (Figure 5). At multiday time scales, the Craig-Gordon model is consistent with the LEL if we use this oceanic kinetic factor instead of the LK value of 14.2‰ (Figure 6). At the annual time scale, the lake evaporation flux calculated with the isotopic mass balance is too low if the LK value is used and is in much better agreement with the eddy covariance evaporation flux if the smaller OS kinetic value is used (Figure 7). Low biases are also seen in the evaporation rate estimated for the Great Lakes using the LK ϵ_k (Jasechko et al., 2014), although they are not as severe as in the present study because HDO was used as an additional tracer to constrain the mass balance of those lakes.

On the other hand, other studies have shown that the lake evaporation flux based on the isotopic mass balance method is in good agreement with that derived from the lake water balance (Gibson et al., 1996, 1998), the Bowen ratio method (Gibson et al., 1996), the two-point aerodynamic profile method (Gibson et al., 1996), a mass transfer approach (Isokangas et al., 2015; Yang et al., 2016), an evaporation pan measurement (Gibson et al., 1998), and the Penman combination method (Gibson et al., 1998; Gibson & Reid, 2014). Most of these studies deploy the commonly used LK ϵ_k values of 14.2‰ for $H_2^{18}O$, and the humidity adjustment factor θ is unity. The isotope calculator of *Hydrocalculator* also uses the standard LK ϵ_k value to describe the kinetic fractionation effect of lake evaporation and a default value of 1 for θ (Skrzypek et al., 2015). The lakes in the experimental studies cited here are much smaller (area less than 2 km²) than Lake Taihu, raising the possibility that large lakes, such as Lake Taihu, behave like the open ocean but small lakes do not.

One explanation why the LK ϵ_k value yields satisfactory results in previous published studies but not for Lake Taihu is that air over small lakes may be less turbulent than that over large lakes because wind speed at small lakes is expected to be weaker due to fetch consideration (Schertzer et al., 2003). However, the kinetic factor is not very sensitive to wind speed, varying only slightly, from 6.9‰ at 10 m s⁻¹ to 6.0‰ at 3 m s⁻¹, according to the theory of Merlivat and Jouzel (1979). The Dalton number of evaporation, a measure of the intensity of turbulent exchange of water vapor between the water surface and the overlying air layer, does not seem to depend on lake size either (Wei et al., 2016; Xiao et al., 2013). Therefore, factors other than levels of turbulence, such as the compensating effect noted below, may be a more plausible explanation for why the LK ϵ_k works in some situations but not in others.

To further address the question as to whether the result presented in section 3 holds for small lakes, we have also analyzed the data collected under short-fetch conditions, with wind blowing from the north shore of the lake (wind direction 315–135°; Figure 1). Because of the short-fetch distance (200–450 m), the air arriving at the measurement platform basically retained the land influences as would be expected of small lakes. The LK parameterization results (Figure S7 in the supporting information) have essentially the same bias errors as in Figures 5 and 6. A comparison between Figure 5 (open fetch) and Figure S7 in the supporting information (short fetch) suggests that the effective ϵ_k was not very sensitive to fetch.

In most of the lake isotopic mass balance studies cited above, the vapor $^{18}O/^{16}O$ was derived from the isotopic equilibrium relationship with precipitation. Direct vapor isotope measurements show that this relationship is most accurate during actual precipitation events (Lee et al., 2006) but may cause high biases during the peak evaporation season (Krabbenhoft et al., 1990). Because the humidity variable h is measured over

the land adjacent to the lake, some researchers have to deploy an empirical factor in the Craig-Gordon model calculation to correct for the advection effect (Bowen et al., 2012; Gat et al., 1994). In such cases, using the standard LK ϵ_k might compensate for biases in the derived vapor isotope ratio and the applied empirical advection factor.

5. Conclusions

A long-standing problem in isotope hydrology has been the disagreement between terrestrial hydrologists and GCM modelers regarding the H_2^{18}O fractionation strength of open-water evaporation. Our results are in agreement with the parameterization used by GCMs for ocean evaporation indicating a weak kinetic effect. The success of the OS ϵ_k at Lake Taihu implies that atmospheric turbulence plays similar roles in gaseous diffusion over the lake and the marine environment. The isotopic mass balance calculations using the weak ϵ_k point to a much stronger role of lake evaporation in the terrestrial hydrological cycle than indicated by previous studies. The annual evaporation rate of Lake Taihu is 520 mm if the LK ϵ_k is used in the isotopic mass balance analysis and increases by 72% to 897 mm if the OS ϵ_k is used. The latter assessment is in better agreement with an independent eddy covariance observation.

An open question is whether the results reported here for a large lake can be extended to small lakes. Possibilities exist that small lakes, being influenced more strongly by air advected from land, may be in a different turbulence regime than large lakes and the open ocean. Although the data obtained under short-fetch conditions suggest that the LK parameterization for ϵ_k may be biased similarly for small lakes, a definite answer will require validation against direct observation of the evaporation isotopic compositions at small lakes.

Acknowledgments

This research was supported by the National Natural Science Foundation of China (grants 41475141 and 41505005), the U.S. National Science Foundation (grant 1520684), the National Key Research and Development Program of China (grant 2016YFC0500102), the Natural Science Foundation of Jiangsu Province, China (grant BK20150900), the Ministry of Education of the People's Republic of China (grant PCSIRT), and the Priority Academic Program Development of Jiangsu Higher Education Institutions (grant PAPD). The data used in this study are available at <http://vapor-isotope.yale.edu/>.

References

- Barkan, E., & Luz, B. (2005). High precision measurements of $^{17}\text{O}/^{16}\text{O}$ and $^{18}\text{O}/^{16}\text{O}$ ratios in H_2O . *Rapid Communications in Mass Spectrometry*, 19(24), 3737–3742. <https://doi.org/10.1002/rcm.2250>
- Benetti, M., Reverdin, G., Pierre, C., Merlivat, L., Risi, C., Steen-Larsen, H. C., & Vimeux, F. (2014). Deuterium excess in marine water vapor: Dependency on relative humidity and surface wind speed during evaporation. *Journal of Geophysical Research: Atmospheres*, 119, 584–593. <https://doi.org/10.1002/2013JD020535>
- Blanken, P. D., Spence, C., Hedstrom, N., & Lenters, J. D. (2011). Evaporation from Lake Superior: 1: Physical controls and processes. *Journal of Great Lakes Research*, 37(4), 707–716. <https://doi.org/10.1016/j.jglr.2011.08.009>
- Bowen, G. J., Kennedy, C. D., Henne, P. D., & Zhang, T. (2012). Footprint of recycled water subsidies downwind of Lake Michigan. *Ecosphere*, 3(6), art53. <https://doi.org/10.1890/ES12-0006.1>
- Cappa, C. D., Hendricks, M. B., DePaolo, D. J., & Cohen, R. C. (2003). Isotopic fractionation of water during evaporation. *Journal of Geophysical Research*, 108(D16), 4525. <https://doi.org/10.1029/2003JD003597>
- Craig, H., & Gordon, L. I. (1965). Deuterium and oxygen 18 variations in the ocean and the marine atmosphere. In E. Tongiorgi (Ed.), *Stable isotopes in oceanographic studies and paleotemperatures* (pp. 9–130). Pisa: Consiglio Nazionale Delle Ricerche Laboratorio di Geologia Nucleare.
- Dee, S., Noone, D., Buening, N., Emile-Geay, J., & Zhou, Y. (2015). SPEEDY-IER: A fast atmospheric GCM with water isotope physics. *Journal of Geophysical Research: Atmospheres*, 120, 73–91. <https://doi.org/10.1002/2014JD022194>
- Dincer, T. (1968). The use of oxygen 18 and deuterium concentrations in the water balance of lakes. *Water Resources Research*, 4(6), 1289–1306. <https://doi.org/10.1029/WR004i006p01289>
- Farquhar, G. D., & Lloyd, J. (1993). Carbon and oxygen isotope effects on the exchange of carbon dioxide between plants and the atmosphere. In J. R. Ehleringer, A. E. Hall, & G. D. Farquhar (Eds.), *Stable isotopes and plant carbon/water relations* (pp. 47–70). San Diego, CA: Academic. <https://doi.org/10.1016/B978-0-08-091801-3.50011-8>
- Garratt, J. R. (1992). *The atmospheric boundary layer*. Cambridge: Cambridge University Press.
- Gat, J. R., Bowser, C. J., & Kendall, C. (1994). The contribution of evaporation from the Great Lakes to the continental atmosphere: Estimate based on stable isotope data. *Geophysical Research Letters*, 21(7), 557–560. <https://doi.org/10.1029/94GL00069>
- Gat, J. R., Klein, B., Kushnir, Y., Roether, W., Wernli, H., Yam, R., & Shemesh, A. (2003). Isotope composition of air moisture over the Mediterranean Sea: An index of the air–sea interaction pattern. *Tellus B*, 55(5), 953–965. <https://doi.org/10.1034/j.1600-0889.2003.00081.x>
- Gibson, J. J., Birks, S. J., Jeffries, D., & Yi, Y. (2017). Regional trends in evaporation loss and water yield based on stable isotope mass balance of lakes: The Ontario Precambrian Shield surveys. *Journal of Hydrology*, 544, 500–510. <https://doi.org/10.1016/j.jhydrol.2016.11.016>
- Gibson, J. J., Birks, S. J., & Yi, Y. (2016). Stable isotope mass balance of lakes: A contemporary perspective. *Quaternary Science Reviews*, 131, 316–328. <https://doi.org/10.1016/j.quascirev.2015.04.013>
- Gibson, J. J., Edwards, T. W. D., Bursey, G. G., & Prowse, T. D. (1993). Estimating evaporation using stable isotopes: Quantitative results and sensitivity analysis for two catchments in northern Canada. *Nordic Hydrology*, 24, 79–94.
- Gibson, J. J., Edwards, T. W. D., & Prowse, T. D. (1996). Development and validation of an isotopic method for estimating lake evaporation. *Hydrological Processes*, 10(10), 1369–1382. [https://doi.org/10.1002/\(SICI\)1099-1085\(199610\)10:10<1369::AID-HYP467>3.0.CO;2-A](https://doi.org/10.1002/(SICI)1099-1085(199610)10:10<1369::AID-HYP467>3.0.CO;2-A)
- Gibson, J. J., & Reid, R. (2014). Water balance along a chain of tundra lakes: A 20-year isotopic perspective. *Journal of Hydrology*, 519, 2148–2164. <https://doi.org/10.1016/j.jhydrol.2014.10.011>
- Gibson, J. J., Reid, R., & Spence, C. (1998). A six-year isotopic record of lake evaporation at a mine site in the Canadian subarctic: Results and validation. *Hydrological Processes*, 12(10–11), 1779–1792. [https://doi.org/10.1002/\(SICI\)1099-1085\(199808/09\)12:10/11<1779::AID-HYP694>3.0.CO;2-7](https://doi.org/10.1002/(SICI)1099-1085(199808/09)12:10/11<1779::AID-HYP694>3.0.CO;2-7)

- Gonfiantini, R. (1986). Environmental Isotopes in Lake Studies. In P. Fritz & J. C. Fontes (Eds.), *Handbook of environmental isotope geochemistry: The terrestrial environment* (Vol. 2, pp. 113–163). Amsterdam: Elsevier.
- Hoffmann, G., Werner, M., & Heimann, M. (1998). Water isotope module of the ECHAM atmospheric general circulation model: A study on timescales from days to several years. *Journal of Geophysical Research*, *103*(D14), 16,871–16,896. <https://doi.org/10.1029/98JD00423>
- Horita, J., Rozanski, K., & Cohen, S. (2008). Isotope effects in the evaporation of water: A status report of the Craig–Gordon model. *Isotopes in Environmental and Health Studies*, *44*(1), 23–49. <https://doi.org/10.1080/10256010801887174>
- Isokangas, E., Rozanski, K., Rossi, P. M., Ronkanen, A.-K., & Kløve, B. (2015). Quantifying groundwater dependence of a sub-polar lake cluster in Finland using an isotope mass balance approach. *Hydrology and Earth System Sciences*, *19*(3), 1247–1262. <https://doi.org/10.5194/hess-19-1247-2015>
- Jasechko, S., Gibson, J. J., & Edwards, T. W. D. (2014). Stable isotope mass balance of the Laurentian Great Lakes. *Journal of Great Lakes Research*, *40*(2), 336–346. <https://doi.org/10.1016/j.jglr.2014.02.020>
- Jasechko, S., Sharp, Z. D., Gibson, J. J., Birks, S. J., Yi, Y., & Fawcett, P. J. (2013). Terrestrial water fluxes dominated by transpiration. *Nature*, *496*(7445), 347–350. <https://doi.org/10.1038/nature11983>
- Jouzel, J., Delaygue, G., Landais, A., Masson-Delmotte, V., Risi, C., & Vimeux, F. (2013). Water isotopes as tools to document oceanic sources of precipitation. *Water Resources Research*, *49*, 7469–7486. <https://doi.org/10.1002/2013WR013508>
- Jouzel, J., Masson-Delmotte, V., Cattani, O., Dreyfus, G., Falourd, S., Hoffmann, G., ... Wolff, E. W. (2007). Orbital and millennial Antarctic climate variability over the past 800,000 years. *Science*, *317*(5839), 793–796. <https://doi.org/10.1126/science.1141038>
- Kim, K., & Lee, X. (2011). Isotopic enrichment of liquid water during evaporation from water surfaces. *Journal of Hydrology*, *399*(3–4), 364–375. <https://doi.org/10.1016/j.jhydrol.2011.01.008>
- Krabbenhoft, D. P., Bowser, C. J., Anderson, M. P., & Valley, J. W. (1990). Estimating groundwater exchange with lakes 1. The stable isotope mass balance method. *Water Resources Research*, *26*, 2445–2453.
- Lee, J. E., Pierrehumbert, R., Swann, A., & Lintner, B. R. (2009). Sensitivity of stable water isotopic values to convective parameterization schemes. *Geophysical Research Letters*, *36*, L23801. <https://doi.org/10.1029/2009GL040880>
- Lee, X., Kim, K., & Smith, R. (2007). Temporal variations of the $^{18}\text{O}/^{16}\text{O}$ signal of the whole-canopy transpiration in a temperate forest. *Global Biogeochemical Cycles*, *21*, GB3013. <https://doi.org/10.1029/2006GB002871>
- Lee, X., Liu, S., Xiao, W., Wang, W., Gao, Z., Cao, C., ... Zhang, M. (2014). The Taihu Eddy Flux Network: An observational program on energy, water and greenhouse gas fluxes of a large freshwater lake. *Bulletin of the American Meteorological Society*, *95*(10), 1583–1594. <https://doi.org/10.1175/BAMS-D-13-00136.1>
- Lee, X., Sargent, S., Smith, R., & Tanner, B. (2005). In situ measurement of the water vapor $^{18}\text{O}/^{16}\text{O}$ isotope ratio for atmospheric and ecological applications. *Journal of Atmospheric and Oceanic Technology*, *22*(5), 555–565. <https://doi.org/10.1175/JTECH1719.1>
- Lee, X., Smith, R., & Williams, J. (2006). Water vapour $^{18}\text{O}/^{16}\text{O}$ isotope ratio in surface air in New England, USA. *Tellus*, *58B*, 293–304.
- Liu, J., Song, X., Yuan, G., & Sun, X. (2014). Stable isotopic compositions of precipitation in China. *Tellus B*, *66*(1), 22,567. <https://doi.org/10.3402/tellusb.v66.22567>
- Luz, B., Barkan, E., Yam, R., & Shemesh, A. (2009). Fractionation of oxygen and hydrogen isotopes in evaporating water. *Geochimica et Cosmochimica Acta*, *73*(22), 6697–6703. <https://doi.org/10.1016/j.gca.2009.08.008>
- Machavaram, M. V., & Krishnamurthy, R. V. (1995). Earth surface evaporative process: A case study from the Great Lakes region of the United States based on deuterium excess in precipitation. *Geochimica et Cosmochimica Acta*, *59*(20), 4279–4283. [https://doi.org/10.1016/0016-7037\(95\)00256-Y](https://doi.org/10.1016/0016-7037(95)00256-Y)
- Majoube, M. (1971). Fractionnement en oxygene-18 et en deuterium entre l'eau et sa vapeur. *Journal de Chimie Physique*, *68*(7–8), 1423–1436. <https://doi.org/10.1051/jcp/1971681423>
- Mathieu, R., & Bariac, T. (1996). A numerical model for the simulation of stable isotope profiles in drying soils. *Journal of Geophysical Research*, *101*(D7), 12,685–12,696. <https://doi.org/10.1029/96JD00223>
- Merlivat, L., & Jouzel, J. (1979). Global climatic interpretation of the deuterium-oxygen 18 relationship for precipitation. *Journal of Geophysical Research*, *84*(C8), 5029–5033. <https://doi.org/10.1029/JC084iC08p05029>
- Noone, D., & Sturm, C. (2010). Comprehensive dynamical models of global and regional water isotope distributions. In J. B. West, et al. (Eds.), *Isoscapes: Understanding movement, pattern and process on Earth through isotope mapping* (pp. 195–219). Dordrecht: Springer. https://doi.org/10.1007/978-90-481-3354-3_10
- Pfahl, S., Wernli, H., & Yoshimura, K. (2012). The isotopic composition of precipitation from a winter storm—A case study with the limited-area model COSMO_{iso}. *Atmospheric Chemistry and Physics*, *12*(3), 1629–1648. <https://doi.org/10.5194/acp-12-1629-2012>
- Risi, C., Bony, S., Vimeux, F., & Jouzel, J. (2010). Water-stable isotopes in the LMDZ4 general circulation model: Model evaluation for present-day and past climates and applications to climatic interpretations of tropical isotopic records. *Journal of Geophysical Research*, *115*, D12118. <https://doi.org/10.1029/2009JD013255>
- Santos, E., Wagner-Riddle, C., Lee, X., Warland, J., Brown, S., Staebler, R., ... Kim, K. (2014). Temporal dynamics of oxygen isotope compositions of soil and canopy CO₂ fluxes in a temperate deciduous forest. *Journal of Geophysical Research: Biogeosciences*, *119*, 996–1013. <https://doi.org/10.1002/2013JG002525>
- Schertzer, W. M., Rouse, W. R., Blanken, P. D., & Walker, A. E. (2003). Over-lake meteorology and estimated bulk heat exchange of Great Slave Lake in 1998 and 1999. *Journal of Hydrometeorology*, *4*(4), 649–659. [https://doi.org/10.1175/1525-7541\(2003\)004<0649:OMAEBH>2.0.CO;2](https://doi.org/10.1175/1525-7541(2003)004<0649:OMAEBH>2.0.CO;2)
- Scott, R. W., & Huff, F. A. (1996). Impacts of the Great Lakes on regional climate conditions. *Journal of Great Lakes Research*, *22*(4), 845–863. [https://doi.org/10.1016/S0380-1330\(96\)71006-7](https://doi.org/10.1016/S0380-1330(96)71006-7)
- Sherwood, S. C., & Risi, C. (2012). The HDO/H₂O relationship in tropospheric water vapor in an idealized “last-saturation” model. *Journal of Geophysical Research*, *117*, D19205. <https://doi.org/10.1029/2012JD018068>
- Skrzypek, G., Mydlowski, A., Dogramaci, S., Hedley, P., Gibson, J. J., & Grierson, P. F. (2015). Estimation of evaporative loss based on the stable isotope composition of water using *Hydrocalculator*. *Journal of Hydrology*, *523*, 781–789. <https://doi.org/10.1016/j.jhydrol.2015.02.010>
- Steen-Larsen, H. C., Sveinbjörnsdóttir, A. E., Peters, A. J., Masson-Delmotte, V., Guishard, M. P., Hsiao, G., ... White, J. W. C. (2014). Climatic controls on water vapor deuterium excess in the marine boundary layer of the North Atlantic based on 500 days of in situ, continuous measurements. *Atmospheric Chemistry and Physics*, *14*(15), 7741–7756. <https://doi.org/10.5194/acp-14-7741-2014>
- Steffensen, J. P., Andersen, K. K., Bigler, M., Clausen, H. B., Dahl-Jensen, D., Fischer, H., ... White, W. C. (2008). High-resolution Greenland ice core data show abrupt climate change happens in few years. *Science*, *321*(5889), 680–684. <https://doi.org/10.1126/science.1157707>
- Sturm, C., Zhang, Q., & Noone, D. (2010). An introduction to stable water isotopes in climate models: Benefits of forward proxy modelling for paleoclimatology. *Climate of the Past*, *6*(1), 115–129. <https://doi.org/10.5194/cp-6-115-2010>

- Subin, Z. M., Riley, W. J., & Mironov, D. (2012). An improved lake model for climate simulations: Model structure, evaluation, and sensitivity analyses in CESM1. *Journal of Advances in Modeling Earth Systems*, 4, M02001. <https://doi.org/10.1029/2011MS000072>
- Wei, Z., Miyano, A., & Sugita, M. (2016). Drag and bulk transfer coefficients over water surfaces in light winds. *Boundary-Layer Meteorology*, 160(2), 319–346. <https://doi.org/10.1007/s10546-016-0147-8>
- Welp, L. R., Lee, X., Kim, K., Griffis, T. J., Billmark, K. A., & Baker, J. M. (2008). $\delta^{18}\text{O}$ of water vapour, evapotranspiration and the sites of leaf water evaporation in a soybean canopy. *Plant, Cell & Environment*, 31(9), 1214–1228. <https://doi.org/10.1111/j.1365-3040.2008.01826.x>
- Wen, X., Lee, X., Sun, X., Wang, J., Hu, Z., Li, S., & Yu, G. (2012). Dew water isotopic ratios and their relationships to ecosystem water pools and fluxes in a cropland and a grassland in China. *Oecologia*, 168(2), 549–561. <https://doi.org/10.1007/s00442-011-2091-0>
- Wen, X., Lee, X., Sun, X., Wang, J., Tang, Y., Li, S., & Yu, G. (2012). Inter-comparison of four commercial analyzers for water vapor isotope measurement. *Journal of Atmospheric and Oceanic Technology*, 29(2), 235–247. <https://doi.org/10.1175/JTECH-D-10-05037.1>
- Wen, X., Sun, X., Zhang, S., Yu, G., Sargent, S. D., & Lee, X. (2008). Continuous measurement of water vapor D/H and $^{18}\text{O}/^{16}\text{O}$ isotope ratios in the atmosphere. *Journal of Hydrology*, 349(3-4), 489–500. <https://doi.org/10.1016/j.jhydrol.2007.11.021>
- Wen, X., Yang, B., Sun, X., & Lee, X. (2016). Evapotranspiration partitioning through in-situ oxygen isotope measurements in an oasis cropland. *Agricultural and Forest Meteorology*, 230-231, 89–96. <https://doi.org/10.1016/j.agrformet.2015.12.003>
- Xiao, W., Liu, S., Wang, W., Yang, D., Xu, J., Cao, C., ... Lee, X. (2013). Transfer coefficients of momentum, heat and water vapour in the atmospheric surface layer of a large freshwater lake. *Boundary-Layer Meteorology*, 148(3), 479–494. <https://doi.org/10.1007/s10546-013-9827-9>
- Xiao, W., Wen, X., Wang, W., Xiao, Q., Xu, J., Cao, C., ... Lee, X. (2016). Spatial distribution and temporal variability of stable water isotopes in an large and shallow lake. *Isotopes in Environmental and Health Studies*, 52(4-5), 443–454. <https://doi.org/10.1080/10256016.2016.1147442>
- Yakir, D., & Sternberg, L. (2000). The use of stable isotopes to study ecosystem gas exchange. *Oecologia*, 123(3), 297–311. <https://doi.org/10.1007/s004420051016>
- Yang, Y., Wu, Q., Yun, H., Jin, H., & Zhang, Z. (2016). Evaluation of the hydrological contributions of permafrost to the thermokarst lakes on the Qinghai-Tibet Plateau using stable isotopes. *Global and Planetary Change*, 140, 1–8. <https://doi.org/10.1016/j.gloplacha.2016.03.006>